g-Values as a Probe of the Local Protein Environment: High-Field EPR of Tyrosyl Radicals in Ribonucleotide Reductase and Photosystem II

Sun Un,*,† Mohamed Atta,‡,§ Marc Fontecave,‡ and A. William Rutherford†

Contribution from the Section de Bioénergétique, URA1290 CNRS, Départment Biologie Cellulaire et Moléculaire, CEA Saclay, F-91191 Gif-sur-Yvette, France, and the Laboratoire d'Etude Dynamiques et Structurales de la Sélectivité, URA332 CNRS, Université Joseph Fourier, F-38041 Grenoble, France

Received April 28, 1995[⊗]

Abstract: The stable tyrosyl radicals in *E. coli* ribonucleotide reductase (RNR) and photosystem II (PSII) were studied by high-field 245 GHz 8.7T EPR. The relaxation properties of Tyr-D°, the stable radical in PSII, are different depending on the spin-state of the manganese-cluster within the protein. Microwave power studies indicated that at high fields and low temperatures the RNR radical relaxes comparably to Tyr-D° when the Mn-cluster is in the paramagnetic state. This verified the existence of a weak exchange coupling between the tyrosyl radical and the nearby binuclear iron site in RNR. A detailed study of the *g*-values of the two radicals was carried out, and these *g*-values were compared to those obtained from an existing 9 GHz single-crystal EPR study of a model tyrosyl radical. The *g*-values of the radicals were calculated using the unrestricted Hartree−Fock MNDO molecular orbital method with PM3 parameterization and the theory of *g*-values of radicals developed by Stone. The spin-orbit coupling contribution to the *g*-values were evaluated using a modified version of Roothaan's theory of electronic excitation. The local environment of the radicals were incorporated into these calculations by inclusion of point charges and hydrogen bonds. The method described here is independent of adjustable parameters except those inherent to the PM3-MNDO method. The calculated *g*-values were in good agreement with those measured experimentally. The differences in *g*-tensors of the tyrosyl radical in RNR, PSII, and the model system are explained in terms of stabilization of the nonbonding orbitals of the tyrosyl oxygen by electrostatic and hydrogen-bonding interactions. The *g*-value calculations also indicate that Tyr-D° is less strongly hydrogen-bonded than in the model system. By incorporating existing ENDOR data into our analysis, we have been able to localize the hydrogen-bond donor to Tyr-D° relative to the phenyl-ring: a hydrogen bond distance of ~1.7 Å, bond angle of ~140°, and dihedral angle of ~35°. This approach which combines high-field EPR measurements of *g*-values with molecular orbital calculations is generally applicable to organic radicals.

Introduction

Since the discovery of the existence of a tyrosyl radical cofactor in *E. coli* ribonucleotide reductase (RNR),[1] a growing number of proteins have been identified which have amino-acid radicals.[2] An important question is how these reactive species are maintained and stabilized within proteins. The tyrosyl radicals in RNR and photosystem II (PSII) are extremely stable despite their high oxidizing potential.[3,4] In the case of PSII the situation is more intriguing since the stable tyrosyl radical, Tyr-D°, does not participate in the electron transfer process, while a second tyrosyl radical, Tyr-Z° is a short-lived electron carrier.[1] Moreover, current structural models of PSII place these tyrosyl radicals in symmetry related positions, one on each subunit of the PSII reaction center heterodimer.[5] Hence, the local environment must play an important role in determining the stability of these tyrosines and their functions.

EPR and ENDOR spectroscopies have played a critical role in the physico-chemical characterization of amino-acid radicals. The tyrosyl radicals have been studied extensively in proteins and model systems. The 9 GHz EPR spectra of these tyrosyl radicals are remarkably varied.[6−8] A strong β-proton nuclear-electron hyperfine coupling, the magnitude of which is determined by the orientation of the β-proton to the phenyl-ring plane (Figure 1), dominates the appearance of the spectra. The EPR spectra of the RNR and PSII tyrosyl radicals are completely different from each other for this reason.[7] Variations in the EPR spectra of tyrosyl radicals in mutants of PSII[9] and RNR[10] have been reported and attributed to changes in proton hyperfine

† CEA Saclay.

‡ Université Joseph Fourier.

§ Current address: Laboratoire de Chimie Organique Biologique, 4, Place Jussieu, Université Paris VI, Tour 214-45, F-75005 Paris Cedex, France.

⊗ Abstract published in *Advance ACS Abstracts,* October 1, 1995.

(1) Larsson, Å.; Sjöberg, B.-M. *EMBO J.* **1986**, *5*, 2037−2040.

(2) Pedersen, J. Z.; Finazzi-Agrò A. *FEBS Lett.* **1993**, *325*, 53−58. Reichard, P. *Science* **1993**, *260*, 1773−1777. Barry, B. A. *Photochem. Photobiol.* **1993**, *57*, 179−188. Stubbe, J. *Ann. Rev. Biochem.* **1989**, *58*, 257−285. Stubbe, J. *Biochemistry* **1988**, *27*, 3893−3900.

(3) Babcock, G. T.; Barry, B. A.; Debus, R. J.; Hoganson, C. W.; Atamian, M.; MacIntosh, L.; Sithole, I.; Yocum, C. F. *Biochemistry* **1989**, *28*, 9558−9565.

(4) Atkins, C. L.; Thelander, L.; Reichard, P.; Lang, G. *J. Biol. Chem.* **1973**, *284*, 7464−7472.

(5) Michel, H.; Deisenhofer, J. *Biochemistry* **1988**, *27*, 1−7. Svenson, B.; Vass, I.; Cedergren, E.; Strying, S. *EMBO J.* **1990**, *9*, 2051-2059. Svenson, B.; Strying, S. *Z. Naturforsch.* **1991**, *46c*, 765−776. Ruffle, S. V.; Donnelly, D.; Blundell, T. L.; Nugent, J. H. A. *Photosyn. Res.* **1992**, *34*, 287−300.

(6) Lassmann G.; Odenwaller R.; Curtis, J. F.; DeGray, J. A.; Mason, R. P.; Marnett, L. J.; Eling, T. E. *J. Biol. Chem* **1991**, *266*, 20045−30055.

(7) Hoganson, C. W.; Babcock, G. T. *Biochemistry* **1988**, *27*, 5848-5855.

(8) Galli, C.; Atta, M.; Andersson, K. K.; Gräslund, A.; Brudvig, G. W. *J. Am. Chem. Soc.* **1995**, *117*, 740−746.

(9) (a) Tommos, C. ; Madsen, C.; Styring, S.; Vermass, W. F. J. *Biochemistry*, **1994** *33*, 11805−11813. (b) Tommos, C.; Davidsson, L.; Svensson, B.; Madsen, C., Vermass, W. F. J.; Styring, S. *Biochemistry* **1993**, *32*, 5436−5441.

(10) Ormö, M.; Regnström, K.; Wang, Z.; Lawrence, Q.; Sahlin, M.; Sjöberg, B.-M. *J. Biol. Chem.* **1995**, *270*, 6570−6576.

0002-7863/95/1517-10713$09.00/0

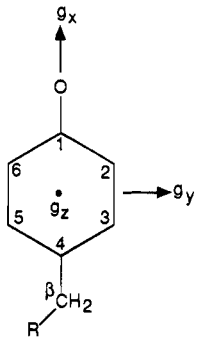

Figure 1. The orientation of the g-tensor in tyrosyl radicals as determined by Fasanella and Gordy[44] from a single crystal study of γ-irradiated tyrosine hydrochloride and the ring numbering scheme.

couplings reflecting structural changes. The electronic spin-density distributions of tyrosyl radicals have been measured by ENDOR[7,11,12] and by pulsed-EPR.[13,14] In PSII, these techniques have characterized the proximal protons to Tyr-D° which are likely candidates as hydrogen-bond donors.[7,13-15]

With the advent of high-field EPR, another important property of amino-acid radicals has become accessible, namely their g-tensors. One of the key driving forces in the development of high-field EPR has been the ability to measure accurately the small g-anisotropies that characterize most organic radicals.[16] Accurate g-values of radicals in biological systems have been measured.[17-21] Un and co-workers demonstrated that the g-anisotropy of the Tyr-D° can be exploited to resolve anisotropic dipolar spin-relaxation from which the relative angular orientation of two paramagnetic species can be derived.[17] By combining distance information obtained from pulse-EPR measurements they were able to determine long-range three-dimensional structural information about PSII. g-Values have also been used to determine detailed information about the radicals themselves and their local structure. Burghaus and co-workers have measured semiquinone radical spectra at 94 GHz.[21] They unambiguously assigned the orientation of the hyperfine tensor relative to the g-tensor. The theory of g-tensors for radicals developed by Stone[22] was used to determine the orientation of the g-tensor relative to the molecular frame. Using simple point-charges to mimic environmental effects, they were also able to rationalize the g-values of quinones.

In this work, we have measured the g-tensors of the tyrosyl radicals in RNR and photosystem II at 8.7 T and 245 GHz. A study of the saturation properties of the EPR signals of these radicals was carried out. In order to understand the differences in the g-values of these tyrosyl radicals and their dependence on their structure and local environment, we have carried out a detailed theoretical analysis of the g-values of tyrosyl radicals. We used the known structures of the RNR protein[23] and of tyrosine hydrochloride.[24] We applied the theory of Stone,[22] with modifications, and calculated g-tensors using a minimal number of approximations and assumptions. By comparing these calculations to experimentally determined g-values, we have been able to elucidate how the local electronic environment around tyrosyl radicals influence the g-tensor. More generally, g-tensors are shown to be effective probes of the local electronic environment. We have extended our analysis to PSII, the structure of which is unknown. The g-values of Tyr-D° provide structural information regarding the hydrogen-bonding to the phenolic oxygen.

Material and Methods

Samples. PSII-enriched membranes were prepared from spinach by the method of Berthold *et al.*[25] with minor modifications. Samples (300 μL) at concentration of approximately 5 mg Chl/mL in a buffer containing 400 mM sucrose, 20 mM MES pH 6.5, and 5 mM $MgCl_2$ were put into a Teflon cup (10 mm in height and 7 mm internal diameter) which acted as the sample holder. They were dark-adapted for a minimum of 30 min and then placed into the cryostat and frozen at zero magnetic field. Illumination of these samples was carried out at 200 K using a 1 mW helium-neon laser for a minimum of 30 min.

Active RNR R2 protein was prepared from the overproducing *E. coli* C600/pBS1 strain.[26] The R2 protein had a specific activity of 4000, 3.2 Fe ions per R2 subunit, and 1 tyrosine per R2 subunit. Protein concentration was determined colorimetrically using bovine serum albumin as a standard[27] and from the absorbance at 280 nm using a molar extinction coefficient of 120 000 M^{-1} cm^{-1}.[28] The 300 μL EPR sample, which was placed in the Telfon cup as described above, contained approximately 116 μM tyrosyl radical, 100 mM Tris-Cl pH 7.5, and 20% (v/v) glycerol. Glycerol was used to stabilize the protein and for good glass formation upon freezing.

Spectrometer. The High Magnetic Field Laboratory EPR spectrometer has been previously described.[29] All spectra were recorded at 245 GHz and 4.2 K. The absolute uncertainty in g-value measurements was estimated to be $\pm 2 \times 10^{-4}$. The large uncertainty results from systematic errors due to magnet field calibration and control. For a given sample, the spectra were reproducible to within $\pm 2 \times 10^{-5}$ in terms of g-values. In principle, a standard of known g-value could be used to lower the absolute uncertainty. The theoretically calculated g-values differ from the measured by about the same amount as the absolute uncertainity. Hence, the results presented here, which relate to the calculations, are not significantly affected.

Calculations. The molecular orbital calculations were carried out using a modified version of MOPAC 6.0[30] on a SUN Microsystems SparcStation 2 and IPC. The modifications permitted the creation of a file which contained various intermediate results of the MNDO calculation needed for subsequent calculations. Calculations of g-tensors were carried out on the same computers using locally written programs. Molecular structures were obtained from the Brookhaven

(11) Rigby, S. E. J.; Nugent, J. H. A.; O'Malley, P. J. *Biohemistry* **1994**, *33*, 1734-1742.
(12) Bender, C. J; Sahlin M.; Babcock, G. T.; Barry, B. A.; Chandrashekar, T. K.; Salowe, S. P.; Stubbe, J.; Lindström, B.; Petersson, L.; Ehrenberg, A.; Sjöberg, B.-M. *J. Am. Chem. Soc.* **1989**, *111*, 8076-8083.
(13) Warncke, K.; Babcock, G. T.; McCracken J. *J. Am. Chem. Soc.* **1994**, *116*, 7332-7340.
(14) Evelo, R. G., Dikanov, S. A.; Hoff, A. J. *Chem. Phys. Lett.* **1989**, *159*, 25-30.
(15) Tang, X.-S; Chisholm, D. A.; Dismukes, G. C.; Brudvig, G. W.; Diner, B. A. *Biochemistry* **1993**, *32*, 13742-13748.
(16) For example, see: Grinberg, O. Y.; Dubinskii, A. A.; Shuvalov, V. F.; Oramskii, L. G.; Kurochkin, V. I.; Lebedev, Y. S. *Dokl. Phys. Chem.* (Eng. Transl.) **1976**, *230*, 923.
(17) Un, S.; Brunel, L.-C.; Brill T.; Zimmermann, J.-L.; Rutherford, A. W. *Proc. Natl. Acad. Sci. U.S.A.* **1994**, *91*, 5262-5266.
(18) Gerfen, G. J.; Bellew, B. F.; Un, S.; Bollinger, J. M.; Stubbe, J.; Griffin, R.G.; Singel, D. J. *J. Am. Chem. Soc.* **1993**, *115*, 6420-6421.
(19) Prisner, T. F.; McDermott, A. E.; Un, S.; Norris, J. R.; Thurnaur, M. C.; Griffin, R. G. *Proc. Natl. Acad. Sci. U.S.A.* **1993**, *90*, 9485-9488.
(20) Gulin, V. I.; Dikanov, S. A.; Tsvetko, Y. U.; Evelo, R. G.; Hoff, A. J. *Pur. Appl. Chem.* **1992**, *64*, 903-906.
(21) Burghaus O.; Plato M.; Rohrer, M.; Möbius, K.; MacMillian, F.; Lubitz, W. *J. Phys. Chem.* **1993**, *97*, 7639-7647.
(22) (a) Stone, A. J. *Proc. Roy. Soc. A* **1963**, *271*, 424-434. (b) Stone, A. J. *Molec. Phys.* **1963**, *6*, 509-515. (c) Stone, A. J. *Molec. Phys.* **1964**, *7*, 311-316.
(23) Nordlund, P.; Sjöberg, B.-M.; Eklund, H. *Nature* **1990**, *345*, 593-598. Nordlund, P.; Eklund, H. *J. Mol. Biol.* **1993**, *232*, 123-164.
(24) Frey, M. N.; Koetzle, T. F.; Lehmann, M. S.; Hamilton, W. C. *J. Chem. Phys.* **1973**, *58*, 2547-2556.
(25) Berthold, D. A.; Babcock, G. T.; Yocum, C. F. *FEBS. Lett.* **1981**, *134*, 231-234.
(26) Sjöberg, B.-M.; Hahne, S.; Karisson, M.; Jörnvall, H.; Göransson, M.; Uhlin, B. E. *J. Biol. Chem.* **1986**, *261*, 5658-5662.
(27) Bradford, M. M. *Anal. Biochem.* **1976**, *72*, 248,254.
(28) Sahlin, M.; Sjöberg, B.-M.; Backer, G.; Loeher, T. M.; Sanders-Loehr, J. *Biochem. Biophys. Res. Comm.* **1990**, *167*, 813-818.
(29) Muller F.; Hopkins, M. A.; Coron, N., Grynberg M.; Brunel, L.-C.; Martinez, G. *Rev. Sci. Instr.* **1989**, *60*, 3681-3684.
(30) Stewart, J. J. P. *MOPAC, A Semi-Empirical Molecular Orbital Program*; QCPE *455*, 1983.

Protein Data Bank and the Cambridge Structure Database. The programs Sybyl (version 6.1) and Pluto (version 5.7) were used to measure structural parameters.

Theory

g-Tensor Calculations. The theory of *g*-tensors of organic radicals was first developed by Stone.[22] A simplified treatment can be found in various textbooks.[31] It can be shown that a particular element of a *g*-tensor arises from three contributions: a relativistic mass correction to the Zeeman energy; the coupling of the electron spin to diamagnetic current induced by the magnetic field; and the spin-orbit coupling. When the unpaired electron resides in a molecular orbital which is characterized by π-type bonding, the relativistic term is essentially a negative shift of the average *g*-value[32] and the diamagnetic current term contributes a positive shift.[22] For the tyrosyl radicals, the first two terms are small compared to the third (see below). The spin-orbit term couples the ground state singly occupied molecular orbital (SOMO) to an excited state SOMO. This spin-orbit contribution to an element of the *g*-tensor is given by

$$g_{ab}^{so} = g_e \mu_B^2 \left(\sum_{n \neq S} \frac{\langle \Psi_S | \xi(r) L_a S_a | \Psi_n \rangle \langle \Psi_n | L_b | \Psi_S \rangle}{E_S - E_n} \right) \quad (1)$$

where g_e is the free electron *g*-value, μ_B the Bohr magneton, Ψ_s the ground state SOMO, Ψ_n all the possible excited state SOMOs, E_s and E_n are the respective energies of the SOMOs, $\xi(r)$ the spin-orbit coupling function, L_a and L_b the orbital angular momentum operators, and S_a the spin angular momentum operator. Angslt has succinctly expressed the relevant equations within the context of the linear combination of atomic orbitals (LCAO) approximation.[32] Typically, $\xi(r)$ is approximated by the spin-orbit coupling constant for each atom. The simplest estimate of the energy difference ($E_s - E_n$) is the difference in the ground state molecular orbital energies ($e_s - e_n$) of the corresponding SOMOs in the ground and excited states. This is known to be a poor approximation to the actual energy difference since the energy of a particular orbital is determined specifically for the ground state configuration of electrons.[33,34] Differences in exchange and coulombic interactions between the ground and excited states must be considered.[34,35] The theory for estimating such effects was first developed by Roothaan.[34] McCain and Hayden[35] Morikawa and Kikuchi[36] have incorporated this theory into their restricted Hartree–Fock calculations of *g*-factors.

Here, we have used the unrestricted Hartree–Fock MNDO (UHF-MNDO)[37] method with PM3 parameterization[38] to calculate the molecular orbitals and the orbital energies necessary to evaluate eq 1. The expressions used to calculated the *g*-tensors were formally identical to those of Angstl.[32] All excited states corresponding to the excitation of either an electron from a doubly occupied level to the SOMO or the SOMO electron to an unoccupied level were used in calculating eq 1.

Only one-center exchange, coulombic and overlap integrals were considered for the *g*-value calculations. This approximation was at a lower level than the MNDO method used for the calculations of the orbitals and their energies. The inclusion of two-center overlap integrals did not appreciably affect the *g*-tensor calculations. The values of all integrals were obtained directly from the MOPAC program.[30]

We derived estimates of the energy difference between the spin-orbit coupled states using the theory of Roothaan.[34] To show the relationship between Roothaan's results and our results, we consider the term which corresponds to the coupling of the ground-state SOMO with an excited state SOMO originating from a doubly filled-orbital in the ground-state, symbolically represented by

$$|\alpha_n\rangle|\beta_n\rangle|\alpha_p\rangle \rightarrow |\alpha_n\rangle|\alpha_p\rangle|\beta_p\rangle$$

where the *n*th level is doubly filled and the *p*th is the SOMO in the ground state and the α and β spin-states are shown to occupy different orbitals, a consequence of the unrestricted Hartree–Fock formalism. The energy difference between these states is given by

$$E_n - E_p = e_n - e_p - J_{pn}^{\beta\beta} + K_{pn}^{\beta\beta} - J_{pn}^{\beta\alpha} + J_{pn}^{\alpha\beta} \quad (2)$$

where E_n and E_p represent the energies of the excited and ground state, and e_n and e_p correspond to the ground state orbital energies of orbitals *n* and *p*. In eq 2, the coulomb integrals, *J*, and exchange integral, *K*, are denoted for the specific spin-state. If the $J_{pn}^{\alpha\beta}$ and $J_{pn}^{\beta\alpha}$ are equal, as would be the case in the restricted Hartree–Fock treatment, then eq 2 would be equivalent to the result obtained by Roothaan.

Structure of Model Systems. No detailed experimental data exists on the structure of tyrosyl radicals. The structures used in our calculations were taken from several *ab initio* geometry optimization calculations.[39] The main difference in these *ab initio* calculations was the C–O bond length which varied from 1.24 to 1.29 Å depending on the basis-set and on the level of the calculation. Bond lengths of this size are between the quinone-like C=O and phenol-like C–O, corresponding to partial conjugation of the C–O bond into the aromatic π-system of the ring. To minimize the number of adjustable parameters and to simplify comparisons between calculations, a single C-O bond length of 1.25 Å was used in all our calculations. *g*-Values calculated using this particular bond length yielded the best agreement with the experimental data (see below). Changes in bond lengths of ±0.01 Å did not yield significantly different *g*-values. It is well-known that hydrogen bonding to a carbonyl group induces changes in the stretching mode of the C–O[40] bond. However these effects are small and any associated changes in the C–O bond length would also be expected to be small. The calculated *g*-values were insensitive to small variations in the bond lengths and angles of the phenyl ring.

Results and Discussion

High-Field EPR Spectra of Tyrosyl Radicals from PSII and RNR. The line shape observed for Tyr-D° of PSII has been previously discussed (Figure 2C).[17] The amplitude distortion was attributed to anisotropic dipolar relaxation effects due to the presence of the Mn-cluster in the paramagnetic (S_2) state. When the manganese cluster was in the diamagnetic (S_1) state,

(31) For example, see: Carrington, A.; McLachlan, A. D. *Introduction to Magnetic Resonance*; Chapman and Hall: London, 1979; pp 134–136.
(32) Angstl, R. *Chem. Phys.* **1989**, *132*, 435–442.
(33) Pople, J. A.; Beveridge, D. L. *Approximate Molecular Orbital Theory*; McGraw-Hill: New York, 1970; pp 31–56.
(34) Roothaan, C. C. J. *Rev. Mod. Phys.* **1951**, *23*, 69–89.
(35) McCain, D.,C.; Hayden, D. W. *J. Magn. Reson.* **1973**, *12*, 312–330.
(36) Morikawa T.; Kikuchi, O. *Theo. Chim. Acta* **1971**, *22*, 224–228.
(37) Dewar, M. J. S.; Thiel, W. *J. Am. Chem. Soc.* **1977**, *99*, 4899–4907.
(38) Stewart, J. P. P. *J. Comput. Chem.* **1989**, *10*, 221–264.
(39) (a) Yu, H.; Goddard, J. D. *J. Mol. Struct. (Theochem)* **1991**, *233*, 129–138. (b) Takahashi, J.; Momosse, T.; Shida, T. *Bull. Chem. Soc. Jpn.* **1994**, *67*, 964–977.
(40) Pinmentel, G. C.; McClellan, A. L. *The Hydrogen Bond*; W. H. Freeman: San Francisco, 1960; pp 255–293.

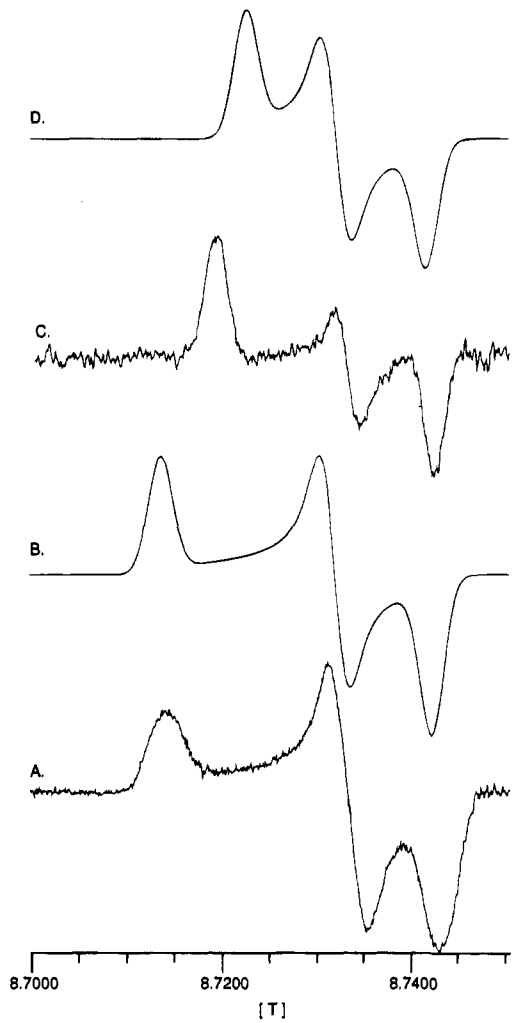

Figure 2. 245 GHz EPR spectra of tyrosyl radicals. The measured spectra of the stable tyrosyl radicals in (A) RNR and (C) PSII. The spectra were obtained at 4.2 K using 15 G and 280 Hz field modulation. (B) The calculated spectrum of the RNR tyrosyl radical based on g-values determined from PM3-MNDO calculations (see text). (D) The calculated spectrum of the tyrosyl radical produced by γ-irradiation of tyrosine hydrochloride based on experimentally measured g-values.[44] The calculated spectra were convoluted with a 10G Gaussian function.

the signal was difficult to observe due to microwave power saturation. The extent of the amplitude distortion can be appreciated by comparison to the spectrum of the tyrosyl radical from ribonucleotide reductase obtained at the same magnetic field (Figure 2A). The latter spectrum can be readily simulated without accounting for relaxation effects (not shown). The g-values of the RNR tyrosyl radical (Table 1) determined from the 245 GHz spectra are consistent with those determined at 140 GHz.[18] The lack of hyperfine resolution in our data is due to the inhomogeneity of the magnet and the frequency instability of the microwave source.

Saturation Properties of the RNR Tyrosyl Radical. Figure 4 shows the amplitude of the EPR signal of the RNR tyrosyl radical and Tyr-D° as a function of microwave power at 4.5K. It should be emphasized that this data is qualitative and that a quantitative comparison of the saturation properties of the RNR and PSII samples would require a careful measurement of the microwave power at the sample. Furthermore, as data is obtained as a function of microwave transmission, the differing compositions of the samples would have to be taken into account. The power indicated on Figure 4 is the relative power that was measured at the far-infrared laser source. Nonetheless, qualitatively the RNR radical relaxes comparably to Tyr-D°

Table 1. Experimental Determined g-Values for Three Tyrosyl Radicals and Calculated PM3-UHF-MNDO g-Values of the Methylphenoxy Radical (pMP) in Various Environments

	g_x	g_y	g_z	g_{av}[a]
Tyr° (RNR) expt	2.00866	2.00423	2.00200	2.00496
pMP isolated	2.0090	2.0045	2.0022	2.0052
pMP − 1 charge[b]	2.0091	2.0045	2.0022	2.0053
pMP all charges[c]	2.0085	2.0045	2.0022	2.0051
pMP +1 charge[d]	2.0086	2.0045	2.0022	2.0051
Tyr° (HCl) expt[e]	2.0067	2.0042	2.0023	2.0045
pMP/AcOH 1.59 Å[f]	2.0066	2.0045	2.0021	2.0044
pMP/AcOH 1.70 Å[g]	2.0074	2.0045	2.0022	2.0047
TyrD° (PSII) expt	2.00745	2.00422	2.00211	2.00459

[a] $g_{av} = {}^1/_3(g_x + g_y + g_z)$. [b] Single negative point charge at 4.6 Å from the oxygen. This models the nearby aspartate group in the RNR. Relative angular placement were taken from the structure (see Figure 3). [c] All nearby charged groups are modeled as point-charges. Relative angular placement were taken for the RNR structure (see Figure 3). [d] Single positive point charge at 6.9 Å from the oxygen which has the equivalent net potential of all the nearby charged groups in RNR structure. [e] Fasanella, E. L.; Gordy, W. *Proc. Natl. Acad. Sci. U.S.A.* **1969**, *62*, 299−304. [f] The relative orientation of the acetic acid molecule relative to the radical was taken from the structure of the diamagnetic tyrosine hydrochloride structure. O···H distance = 1.59. [g] As for *f*, O···H distance = 1.70 Å, CO···H angle = 140°, dihedral angle relative to ring-plane = 30°.

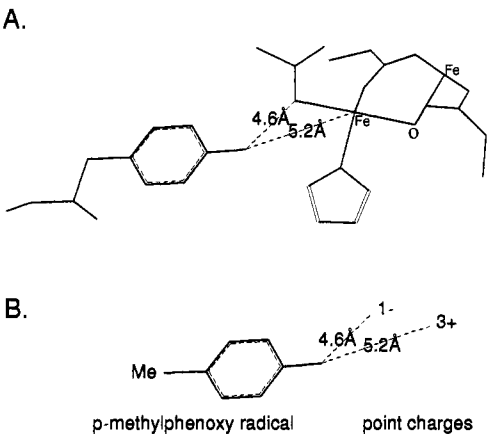

Figure 3. A. The structure of RNR about the tyrosyl radical.[23] The nearest Fe ligands is a glutamate at 3.76 Å from the oxygen. The irons are 5.2 and 8.2 Å away. B. The structure of the *p*-methylphenoxy radical and point charges used to model glutamate and nearest iron in the g-tensor calculations.

when the manganese cluster is in the paramagnetic S_2 state. When the manganese is in the diamagnetic S_1 state, the signal is extremely weak due to saturation. Even at the lowest powers used to obtain the unsaturated S_2 state Tyr-D° signal, the S_1 state Tyr-D° signal was saturated.[17] The crystallographic structure of the RNR protein shows that the nearest iron of the binuclear iron site to be about 5.2 Å away from the tyrosyl radical (Figure 3), and magnetic studies indicate that the metal-center has a spin-less (S = 0) ground state.[41,42] The relatively fast relaxation rate in the RNR case is probably caused by an exchange interaction between the radical and the iron-center. The exchange interaction has been estimated to be 0.0047 cm^{-1} by Hirsch and co-workers.[8,43] Previous 9 GHz variable-temperature EPR studies observed that the radical saturated much more easily as the temperature was decreased, and at temperatures below 10 K the saturation properties became

(41) Sahlin M.; Peterson, L.; Gräslund, A.; Ehrenberg, A.; Sjöberg, B.-M.; Thelander, L. *Biochemistry* **1987**, *26*, 5541−554.
(42) Atta, M.; Scheer, C.; Fries, P. H.; Fontecave, M.; Latour, J.-M. *Angew. Chem., Int. Ed. Engl.* **1992**, *31*, 1513−1515.
(43) Hirsh, D. J.; Beck, W. F.; Lynch, J. B.; Que, L.; Brudvig, G. W. *J. Am. Chem. Soc.* **1992**, *114*, 7475−7481.

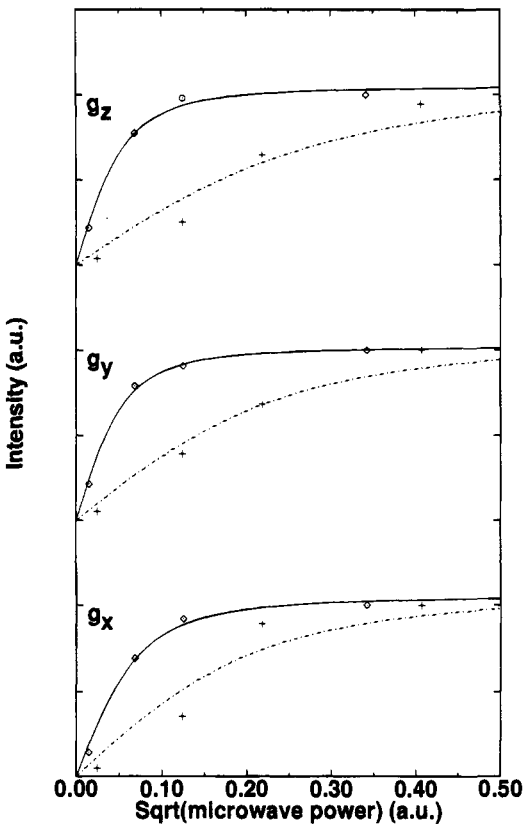

Figure 4. The dependence of signal amplitude of the microwave power for the tyrosyl radicals in PSII (diamond shape with dot, solid-line) and RNR (+, dotted-line) at g_x, g_y, and g_z field positions. For PSII, the manganese cluster was in the S_2 state. When the cluster was in the S_1 state the tyrosyl radical spectrum was saturated at all powers. The data for each g-value has been arbitrarily offset. The lines represent best fit to the equation $A\omega_1 x/\sqrt{1+\omega_1^2 x^2}$ where A is a normalization constant, ω_1 is the square root of the measured power, and x is related to T_1T_2 (Castner, J. G. *Phys. Rev.* **1959**, *115*, 1506−1515).

constant.[41] The high-field observations would appear to be contradictory with these observations. However, the intrinsic relaxation rates of the radicals are likely to be much slower at high-fields and the saturation properties much more sensitive to the magnetic environment. Such enhanced effects at high-field have been previously described for Tyr-D° in PSII.[17]

Qualitative Analysis of *g*-Tensors. Another noticeable difference between the tyrosyl radical spectra (Figure 2) is the difference in the g_x values (low-field edge). This is more striking when compared to the g_x-value of the tyrosyl radical generated from γ-irradiation of tyrosine hydrochloride crystals measured by Fasanella and Gordy.[44] To emphasize this difference a calculated spectrum of this radical is also shown in Figure 2D. The differences in g-values of the tyrosyl radicals can be understood using the same arguments which were used by Stone to rationalize the g-values of semiquinones.[22b] For quinones, the largest contribution to the g-tensor is from the spin-orbit coupling of the ground state SOMO with the excited state SOMO corresponding to a nonbonding orbital. These nonbonding orbitals are characterized by the nonbonding electrons of the oxygen and lie in the plane of the phenyl-ring. Therefore, the spin-orbit contributions are expected to be greatest in the in-plane directions. Therefore, the differences which are seen in Figure 2 must arise from some combination of changes in the SOMO, the nonbonding orbitals, and their respective energies.

(44) Fasanella, E. L.; Gordy, W. *Proc. Natl. Acad. Sci. U.S.A.* **1969**, *62*, 299−304.

As previously mentioned, the structure of the RNR protein has been determined, and the relevant portion of the structure is shown in Figure 3. The tyrosyl radical is relatively isolated within a hydrophobic pocket[10,23] with the nearest iron of a binuclear iron center 5.2 Å away.[23] The structure of PSII is unknown; however, based on spectroscopic evidence it has been proposed that the Tyr-D° is hydrogen-bonded (see below).[7,11,14,15] A neutron diffraction structure of the diamagnetic tyrosine hydrochloride has been determined.[24] In this structure, the phenolic oxygen of each tyrosine molecule is hydrogen-bonded to the proton of the carboxylic group of a neighbor. The proton-oxygen bond distance is 1.6 Å. The tyrosyl radical within the diamagnetic tyrosine hydrochloride crystals is assumed to exist in the same spatial configuration as the host molecules.[44] The g-tensors of the three radicals are entirely consistent with the known structural data described above and eq 1. Hydrogen-bonding lowers the energy of the nonbonding orbitals which increases the energy difference between this orbital and the SOMO which in turn reduces the magnitude of g_x. Therefore, Tyr-D° presents an intermediate situation between the non-hydrogen-bonded case of RNR and the more strongly hydrogen-bonded situation in tyrosine hydrochloride. This g_x-value shift can be explained solely in terms of changes in the nonbonding orbital. In principle, no changes in the ground state SOMO need occur (see below).

Calculation of *g*-Factors. Burghaus and co-workers have studied the high-field EPR spectra of semiquinone radicals and have shown that semiempirical INDO molecular orbital methods can be used to calculate g-tensors and qualitatively explain environmental effects such as solvent hydrogen-bonding.[21] We carried out similar calculations on the tyrosyl radicals. Our calculations differed from those of Burghaus in several ways. We used a higher-level of approximation, namely the MNDO method.[37] The PM3 parameterization[38] which we employed has been shown to be better than the original MNDO parameterization and has been demonstrated to describe hydrogen-bonding more accurately.[38] As described above, our calculations also attempted to determine more accurately the energy difference term in the denominator of eq 1. The basic computational model was the *p*-methylphenoxy radical (pMP). Calculations of the complete tyrosyl radical took more time. The contributions to the g-factor of the amino and carboxyl groups were negligible.

The calculated g-tensor of an isolated pMP radical is shown in Table 1. The structure employed in the calculations was described in the previous section. The calculated orientation of the g-tensor was in agreement with that determined experimentally by Fasanella and Gordy[44] and is shown in Figure 1. The g_x value was dominated by a single term in the spin-orbit contribution (see eq 1) corresponding to the coupling between SOMO and the nonbonding orbital. The spin-orbit contribution to g_x was 0.0068. The next largest contribution was approximately an order of magnitude smaller. The diamagnetic current contribution was 7×10^{-5} in the g_x- and g_y-directions and 3×10^{-5} in the g_z-direction. The relativistic correction was -1.4×10^{-4} in all three directions. The observation that the g_z value is less than the free electron g-values is accounted for by the negative value of the relativistic correction.[32] The calculated g-values for the isolated pMP radical were found to be similar to those of the RNR tyrosyl radical with the g_x value somewhat larger in the hypothetical case. This agreement is most likely fortuitous. In the protein, the charged ferric atoms and their ligands are sufficiently close to interact electrostatically with the tyrosyl oxygen electrons. If the nearby aspartate group is modeled by a single negative point-charge, the calculated g_x-value is 2.0091 (see Table 1, pMP-negative point-charge model).

Inclusion of a triple positive point-charge in order to model the nearest ferric atom, in addition to the negative point charge, yielded a g_x-value calculated to be 2.0081. When all of the charged groups were modeled by point-charges, g_x was 2.0085. The calculated spectrum based on this final model is shown in Figure 2B. Within the point-charge approximation, the net electrostatic potential of all the charge groups was calculated to be approximately equivalent to a single positive point-charge 6.88 Å from the tyrosyl oxygen atom. For this model, the g_x was 2.0086. This calculation demonstrates that a small net electrostatic stabilization of the nonbonding oxygen electrons occurs and decreases the g_x-value relative to the isolated tyrosyl radical.

We also calculated the g-values for the tyrosyl radical produced in tyrosine hydrochloride by γ-irradiation. The model which we employed consisted of a methylphenoxy radical hydrogen bonded to an acetic acid molecule. The hydrogen-bonding geometry (i.e., bond and dihedral angles) was identical to that found in the diamagnetic tyrosine hydrochloride host.[24] The best fit to the experimental g-tensor measured by Fasanella and Gordy[44] was found when the C···HO bond length was set to 1.59 Å with the oxygen−oxygen distance set to that found in the crystallographic structure (2.62 Å). The calculated values differed from the experimental by less than 3×10^{-4} (Table 1). The g-values did not change significantly when the C−O bond length was varied from 1.24 to 1.26 Å.

The tyrosyl radicals produced by irradiation and naturally occurring in the RNR protein are examples of two quite different local electronic environments. By using computational models which incorporate these environmental effects, we are able to calculate g-tensors accurately. It is important to note that unlike previous calculations we did not use arbitrary scaling parameters within the g-factor calculation.[21,45] Aside from the approximations inherent in the semiempirical molecular orbital and g-factor calculations, the only other approximations were those concerning the structure of the radicals (see above) and their local environments. Data on these local environments come from crystallographic studies of the nonradical forms of the RNR protein[23] and tyrosine hydrochloride crystals.[24] However, the consistency between the experimentally measured and calculated g-values appears to justify the use of these structural approximations. We have achieved equally good results with semiquinone radicals and will report on these and other calculations in a subsequent publication.

g-Values of Tyr-D°. Encouraged by the near quantitative agreement between the PM3-MNDO calculated and experimentally determined g-values, we examined in detail the behavior of the g-tensor as a function of the hydrogen-bonding geometry. We used the simple methylphenoxy/acetic acid pair-model and carried out a large number of calculations where the bond distance, bond angle, and dihedral angle with respect to the phenyl-ring plane were systematically varied. For all reasonable bond lengths and angles, the g_y and g_z components did not significantly change. However, the g_x was extremely sensitive. Figure 5 shows the dependence of the g_x values as a function of the hydrogen bond distance. As the hydrogen bond distance varies from 2.00 to 1.55 Å, the g_x value changes from that of the tyrosyl radical in RNR to that of the γ-irradiated tyrosine hydrochloride to even smaller values. Figure 6 summarizes the effect of hydrogen-bond orientation and bond distance. The contours represent values for which g_x is 2.0074, the value for Tyr-D°. At 1.55 Å, two possible sets of orientations were found: the unique bond-angle of 180° and the region where

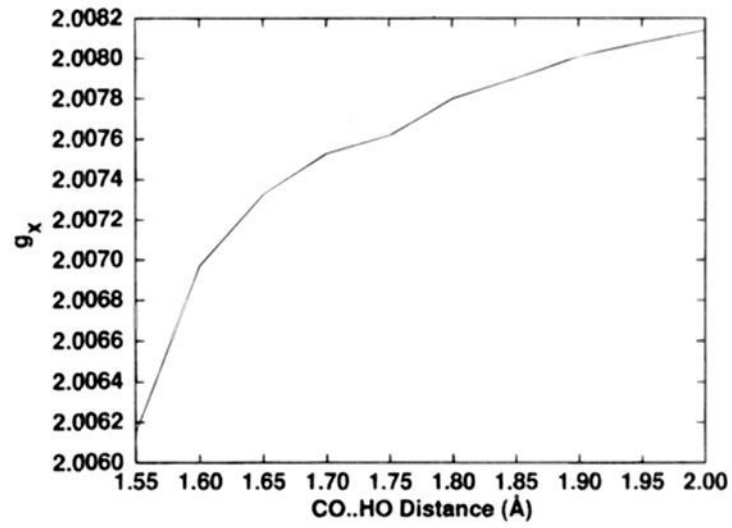

Figure 5. The calculated dependence of g_x on the hydrogen bonding distance for the p-methylphenoxy radical acetic acid pair. The hydrogen bond angle is 140°, and the dihedral angle relative to the ring plane is 30°.

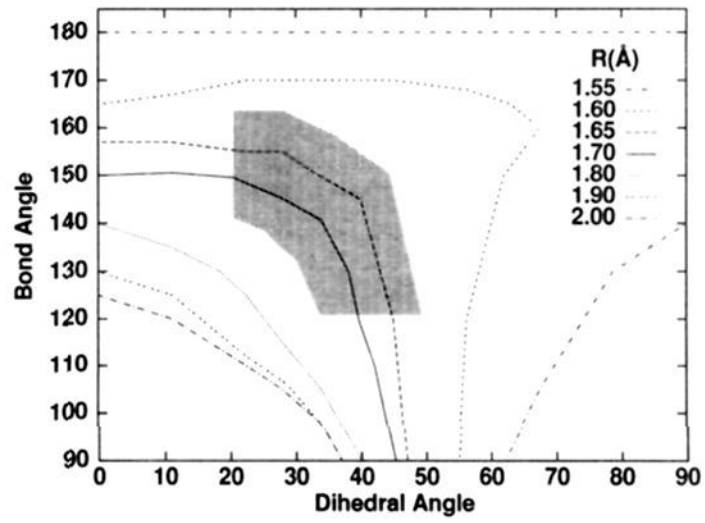

Figure 6. The possible orientation of the p-methylphenoxy radical acetic acid pair which yield g_x value identical to Y_D as a function of distance. When published ENDOR data[7,11,15] and steric hindrance are considered, the possible orientations can be further restricted to the shaded area.

the dihedral angle is near the maximum. At such a short bond distance and large g_x value, the only orientations which are possible are those which would be predicted to make the poorest hydrogen-bond. The possible geometries can be constrained further by considering the published ENDOR data. A 3.5 MHz proton signal has been detected and tentatively assigned to the proton which hydrogen-bonds to Tyr-D°.[7,11,15] Using the method of Hemeka and Turner,[46] we calculated the oxygen spin-density for both the methylphenoxy/acetic acid pair and methylphenoxy-RNR model and determined the spin densities to be 0.22 and 0.24, respectively. These calculated values are in very good agreement with O^{17} ENDOR measurements on isotopically labeled tyrosyl radicals. The measured oxygen spin densities were approximately 0.25 for the radical in RNR and 0.23 for the radical generated by UV irradiation.[47] These densities are also consistent with pulse EPR[13] and other ENDOR[11] studies which determined the combined C(1) and O spin densities to be 0.22 to 0.25 for Tyr-D°. The C(1) spin density is expect to be very low.[44] By applying a simple point dipole approximation, a $A_\perp$ hyperfine component of 3.5 MHz and a spin-density of 0.22, one arrives at a distance of 1.7 Å. At this distance, for small dihedral angles (0°−20°), the hydrogen bond angle was about 150°. For hydrogen bond angles less than 120°, the dihedral angle was 40° to 45°. In these two regions, space filling models show significant steric hindrance from the two *ortho*-position hydrogens and hence make these orientations unfavor-

(45) Chuvylkin, N. D.; Zhidomirov, G. M. *Mol. Phys.* **1973**, *25*, 1233−1235.

(46) Hameka, H. F.; Turner, A. G. *J. Magn. Reson.* **1985**, *64*, 66−75.
(47) Hoganson, C. W.; Babcock, G. T., personal communication.

able. When all of the above information is taken together, the likely orientation of the hydrogen-bond is centered about a bond angle of 140° and dihedral angle of 35°.

Implications to Mutagenesis Studies. Our experimental data and theoretical interpretations have significant implications for spectroscopy carried out at conventional fields. Table 1 indicates that modifications of the local electronic environment, such as changes in hydrogen-bonding induced by site-directed mutagenesis,[9,15] can change the *g*-anisotropy by as much as 2×10^{-3} which corresponds to a change of approximately 3 G at 9 GHz. In particular for mutants of PSII, the interpretation of the EPR spectra of Tyr-D° based solely on hyperfine interaction would seem to be overly simplified.[9a] Changes in *g*-anisotropy could potentially be as large as changes in hyperfine interactions. It is not clear whether simulations of 9 GHz spectra are unique under these conditions and are sufficiently sensitive to distinguish between these changes in *g*-anisotropy and hyperfine interactions.

Site-directed mutagenesis studies of the histidine-189 residue in PSII have been reported.[9b,15] His-189 has been identified as a likely hydrogen-bond donor to Tyr-D°. The EPR spectrum of the His189Gln mutant was less resolved than the wild-type.[15] This is consistent with a weakening of the hydrogen-bond leading to an increase in *g*-anisotropy. The His189Asp mutant yielded a narrower 9 GHz EPR spectrum (approximately 11G). Based on our study, this is exactly the opposite effect that one would expect from the introduction of a negatively charged group. Moreover, it is unlikely that the dominant isotropic hyperfine coupling to the β-protons can be reduced sufficiently, either by rotation or by redistribution of the spin density, to offset the increase in *g*-anisotropy. Existing experimental data[6,7,9a,44] obtained from tyrosyl radicals in a variety of environments indicate that the isotropic hyperfine coupling to the 2,6 position ring protons (see Figure 1) is about 6 to 7 G leading to a triplet resonance, the width of which is 12 to 14 G. The hyperfine couplings to these ring protons are not significantly affected by local environment. Although the minimum hyperfine coupling to a β-proton is zero, there are two such protons which are separated by 120° with respect to the phenyl ring plane. Hence, the minimum contribution from both protons is expected to be at least 5 G. Therefore, the minimum width of a 9 GHz tyrosine spectrum must be at least 17 G. The inclusion of *g*-anisotropy would increase this figure. Hence, the assignment of these narrow signals to tyrosine in these mutants appears to be doubtful.[9b,15]

Spin-Densities and *g*-Values. Stone in his treatment of *g*-tensors of semiquinones noted that the *g*-anisotropy was directly dependent on the electron density on the p_z-orbital of the oxygens.[22b] Subsequent work related the changes in spin-density on the oxygen to changes in the isotropic *g*-values of the semiquinones.[48] Equation 1 and Stone's first observations clearly indicate that this relationship must exist. However, the inverse relationship is not necessarily valid: that is changes in *g*-values need not imply changes in spin densities. In good agreement with O^{17} ENDOR measurements,[47] our calculations predict that the tyrosyl radicals produced by irradiation and in the RNR protein have the same oxygen spin densities to within 10%. However, the same calculations predict a drastic change in *g*-values. In fact, Stone's original observations should be amended to include the fact that semiquinone and tyrosyl *g*-values are also dependent on the nonbonding electron density on the oxygen and their energies. If the local environment principally affects the nonbonding molecular orbital and its energy, as one might expect with hydrogen bonding, then the *g*-values will also change in response to these effects even when the oxygen spin density remains constant or little changed. The earlier interpretation of the differences in the RNR *g*-values compared to those of Tyr-D° is equivocal since the arguments were solely based on oxygen spin density variations.[18] In general, the variations in *g*-values result from simultaneous changes in both the SOMO and the other molecular orbitals to which it is spin-orbit coupled while variations in hyperfine couplings reflect only changes in the SOMO.

Conclusion

We have shown that *g*-values of tyrosyl radicals are a very sensitive probe of the local electronic environment. High-field EPR has made it possible to measure the *g*-values accurately. A quantitative understanding of the differences in the *g*-values of the tyrosyl radicals in γ-irradiated tyrosine hydrochloride and RNR has been obtained using approximate molecular orbital calculations and crystallographic data. These calculations were extended to obtain local structural information concerning Tyr-D° in PSII, the structure of which is unknown. Based on high-field EPR data and molecular orbit calculations, the hydrogen bonding in PSII appears to be weaker than in the γ-irradiated tyrosine hydrochloride with a C−O···H angle of approximately 140° and a dihedral angle relative to the ring plane of approximately 35°. In general, by bringing together accurate *g*-value measurements and molecular orbital calculations, we have shown that detailed information regarding the local bonding and electronic interactions involving radicals in proteins can be obtained. Furthermore, radicals appear to be much more sensitive to the magnetic environment at high-fields, as demonstrated by our study of the saturation properties of the tyrosyl radicals in PSII and RNR and by previous observation on the anisotropic relaxation effects on Tyr-D. Hence, with high-field EPR it is possible to evaluate the local electronic and magnetic environment of radicals providing valuable information regarding the mechanism by which proteins are able to maintain and stabilize highly-reactive radicals.

Acknowledgment. We thank the High Magnetic Field Laboratory for the use of their facilities. Thilo Brill and Louis-Claude Brunel are acknowledged for their assistance in carrying out experiments. We are grateful to Professor G. T. Babcock for sharing his unpublished O^{17} ENDOR results. This research was supported by a grant from the Human Frontiers Science Organization and GDR Metalloproteins program of the CNRS.

JA951377L

(48) Prabhananda, B. S. *J. Chem. Phys.* **1983**, *79*, 5752−5757.